Chinese Chemical Letters 36 (2025) 110000

Contents lists available at ScienceDirect

Chinese Chemical Letters

journal homepage: www.elsevier.com/locate/cclet

Bimetallic composite carbon fiber with persulfate mediation for intercepting volatile organic compounds during solar interfacial evaporation

Yuling Ma, Dongqing Liu, Tao Zhang, Chengjie Song, Dongmei Liu, Peizhi Wang*, Wei Wang*

State Key Laboratory of Urban Water Resource and Environment, School of Environment, Harbin Institute of Technology, Harbin 150090, China

ARTICLE INFO

Article history:
Received 1 February 2024
Revised 9 April 2024
Accepted 10 May 2024
Available online 11 May 2024

Keywords:
Solar distillation
Interfacial evaporation
Volatile organic compounds
Bimetallic composite carbon fiber
Persulfate mediation

ABSTRACT

Solar interfacial evaporation (SIE), is currently one of the most potential water supply technologies in the remote, insular, and disaster-stricken areas. However, the existence of volatile organic compounds (VOCs) in water deteriorates the distillate quality, threatening human health. Herein, we constructed a carbon-based bimetallic (C/FeCo) photothermal membrane by electrospinning technique. Results illustrated that the membrane can catalytically degrade VOCs during SIE with persulfate (PDS) mediation. PDS, as well as phenol, was mainly reacted on the interface of the photothermal membrane instead of in the bulk solution. The interception efficiency of phenol achieved nearly 100% using the C/FeCo membrane during SIE. Hydroxyl radical ($^{\bullet}OH$), sulfate radical ($SO_4^{\bullet-}$), superoxide radical ($O_2^{\bullet-}$), and singlet oxygen ($^1O_2$) were identified as the main active substances to degrade VOCs. We also conducted SIE experiments using actual river water to evaluate the practical performance of the C/FeCo membrane. This work holds the promise of VOCs interception during SIE and enlarges the application of solar distillation in water/wastewater treatment.

Solar interfacial evaporation (SIE), the most efficient technology of solar distillation [1], is currently one of the most hopeful and sustainable water supply strategies in the remote, insular, and disaster-stricken areas where energy lacks [2,3]. During the SIE process, the raw water is lifted to the surface of the photothermal material and heated to vaporize the clean water [4,5]. A solar-thermal material with capabilities of high photothermal conversion and fast water transportation is essential for an efficient and sustainable SIE process [6]. Recently, researchers have developed many strategies, such as *in situ* gelation, to improve the heat absorption [7-9] and water evaporation abilities [10-12] of solar-thermal materials. The photothermal conversion rate of two-dimensional materials can be up to 80%, and the water evaporation rate can achieve nearly 2 kg m^{-2} h^{-1} or higher [13]. However, many feedwater (*e.g.*, surface water and treated wastewater) contain volatile organic compounds (VOCs), which can be evaporated and concentrated in the distilled water during the SIE process, threatening the human health [14,15]. Owing to the lower saturated vapor pressure than that of the water, VOCs can be vaporized with water simultaneously [10,16]. Researchers have developed lots of methods to solve this problem, such as Fenton catalytic oxidation [17], photocatalytic technology [18-21], and selectively permeable photothermal material [22,23]. Nevertheless, the complexity and stability of the processes or the cost-ineffectiveness of materials still restrained the implementation potential of these methods.

The advanced oxidation process with persulfate (PDS) as electron acceptor (SAOP) has become a hot topic in academic and engineering fields [24]. PDS is very stable at ambient temperature and pressure, and can produce hydroxyl radicals ($^{\bullet}OH$) and sulfate radicals ($SO_4^{\bullet-}$) to strongly oxidate organic pollutants under certain conditions. $^{\bullet}OH$ and $SO_4^{\bullet-}$ both have high redox potentials, ranging from 1.9 V to 2.7 V and 2.5 V to 3.1 V, respectively [25]. PDS can be activated by means of light [26], heat [27], transition metal [28], ultrasound [29], or even composite systems [30,31]. With the merits of solar photothermal energy, the SIE system can be a promising choice for activating PDS to remove VOCs [32]. However, only solar-heating SAOP cannot degrade VOCs effectively. A composite system is needed to increase the interception efficiency of VOCs during the SIE process. Carbon-based materials have good photothermal performance and can catalyze the activation of PDS [33].

* Corresponding authors.
E-mail addresses: wangpeizhi827@hotmail.com (P. Wang), wangweirs@hit.edu.cn (W. Wang).

https://doi.org/10.1016/j.cclet.2024.110000
1001-8417/

Given that the transition metals possess high activity for PDS activation, they can be decorated on carbon-based photothermal materials to realize the integration of photothermal and catalytic activation processes in one system [34,35]. During SIE, the raw water with PDS is lifted to the interface of the photothermal material; the radicals can be continuously produced under the activation of thermal energy and catalyst; the VOCs can be quickly degraded, avoiding their volatilization to the distillate. However, the metal elements can be easily leached out from the single metallic catalysis, decreasing the catalytic oxidation effects and shortening the catalyst lifespan [36]. Previous studies have demonstrated that bimetallic combined catalysis could mitigate the metal leaching problem [37]. Integrating solar-thermal materials with bimetallic catalyst might be a promising way to comprehensively improve the performances of the SIE process.

In the present work, we fabricated a stable bimetallic composite carbon fiber using transition metals (Fe and Co), which could effectively intercept the VOCs with PDS mediation and purify water during SIE. The bimetallic (C/FeCo) photothermal membrane showed excellent solar absorption and water evaporation efficiency (1.48 kg m^{-2} h^{-1} under 1 sun). The interception efficiency of volatile phenol for the C/FeCo membrane evaporator kept at nearly 100% under different circumstances (*e.g.*, initial phenol 5–35 mg/L, initial sailinity 0%-3.5%) during evaporation with less oxidant consumption. Electron spin resonance (ESR) was utilized to analyze the catalytic oxidation mechanism of the bimetallic membrane. Hydroxyl radical ($^{\bullet}OH$), sulfate radical ($SO_4^{\bullet-}$), superoxide radical ($O_2^{\bullet-}$), and singlet oxygen ($^1O_2$) were the main active substances in this system. More importantly, when employed to purify practical river water, it effectively degraded complex natural VOCs and the distilled water met the drinking water standards of China. This work holds the promise of VOCs interception during SIE, enlarging the application potential of solar distillation to produce clean water, treat wastewater, *etc.*

To clarify the surface microstructure of the photothermal membranes with catalyst, the relevant samples were measured by scanning electron microscope (SEM). As shown in Figs. 1a–c, Fe and Co elements were successfully loaded on the carbon fibers after dosing ferric chloride and cobalt chloride to the spinning solutions. Compared with C membrane, there are some particles on the surface of the fiber in C/Fe and C/FeCo membranes, and C/FeCo membrane contains more particles. Energy dispersive spectrometer (EDS) mapping images illustrated that Fe and Co elements are distributed evenly on the entire surface of the membrane, which also provides good material support for the catalytic performance. Interestingly, the positions of Fe and Co elements on the surface of the C/FeCo membrane are almost the same, which is basically the position of spherical particles in Fig. 1c. As shown in Fig. 1d, C/FeCo membrane loaded more Fe than C/Fe membrane. Two metal elements on C/FeCo membrane formed some combination, and in the subsequent evaporation experiment, the catalyst may be a mixture or compound of Fe and Co elements. X-ray diffraction (XRD) phase analysis was introduced to analyze the metal element compounds on the composite membrane. As shown in Fig. 1e, there is a weak diffraction peak of Fe_2O_3 (corresponding to PDF #16–0653) on the C/Fe membrane. Notably, C/FeCo membrane shows obvious signal and sharp peaks at 45.112°, 43.871°, and 35.437°, indicating the presence of Fe-Co composite metal compounds (*i.e.*, $Co_{0.7}Fe_{0.3}$ (corresponding to PDF #48–1818), $Co_{0.72}Fe_{0.28}$ (corresponding to PDF #51–0740), and $CoFe_2O_4$ (corresponding to PDF #22–1086)). These indicate that Fe and Co metal compound has good crystallization, which explains the phenomenon that Fe and Co elements appear in the same position in Fig. 1c, and also indicates bi-metal catalyst maintains good stability. Water contact angle tests illustrated that the metal-containing membranes possess higher hydrophilicity (C: 49°, C/Fe: 48°, C/FeCo: 37°, Fig. 1f), favoring its usability for water evaporation.

The evaporation performance (under 1 sun) of the photothermal membranes in this study was shown in Fig. 2. The mass change of the evaporators is linear, implying the stable evaporation process of three systems (Fig. 2a). As shown in Fig. 2b, evaporation rate (ER) of the C membrane is 1.44 kg m^{-2} h^{-1}, which is almost twice than that with no photothermal membrane. ER of the C/Fe membrane (1.17 kg m^{-2} h^{-1}) is lower than that of the C membrane, while the C/FeCo membrane (1.45 kg m^{-2} h^{-1}) shows the highest ER. Full spectra absorption tests (Fig. 2c) illustrated that C/FeCo membrane holds higher solar absorption efficiency (94.58%) than C/Fe membrane (90%), and is almost close to the C membrane (94.99%). According to Fig. 2d, the surface temperature of C/FeCo membrane changed from 20 °C to 41.5 °C, while that of C/Fe membrane changed from 20 °C to 40.3 °C. Thus, the calculated light-to-vapor conversion efficiency of C/FeCo membrane (75.23%) performs a little higher than that of C/Fe membrane (74.53%). These results indicate that the addition of Fe and Co elements to the C membrane have little effects on the evaporation performance of the photothermal membrane.

To evaluate the VOC interception performance of the photothermal membrane in SIE system, phenol was chosen as a model con-

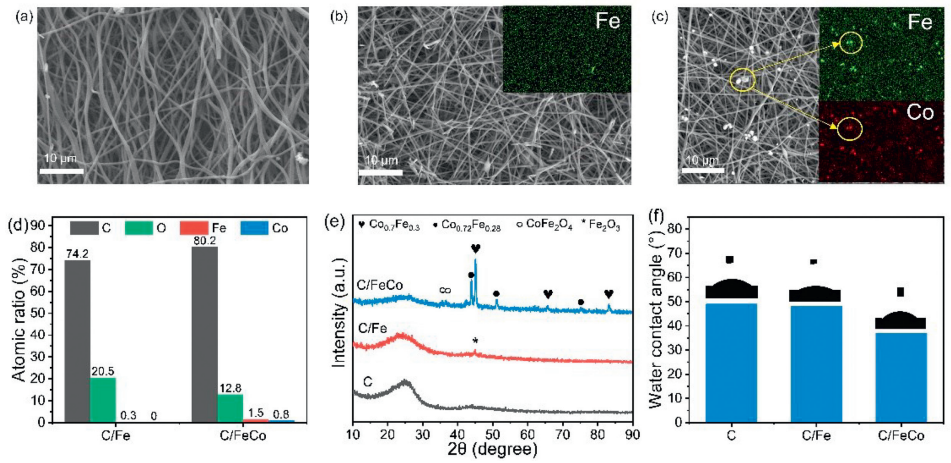

Fig. 1. (a) SEM image of C membrane. (b) SEM image of C/Fe membrane and corresponding EDS mapping of Fe element. (c) SEM image of C/FeCo membrane and corresponding EDS mapping of Fe and Co elements. The positions of Fe and Co elements on the surface of the C/FeCo membrane are almost the same. (d) Atomic ratio of C/Fe and C/FeCo membranes. (e) XRD spectra of C, C/Fe, and C/FeCo membranes. (f) The water contact angle of C, C/Fe, and C/FeCo membranes.

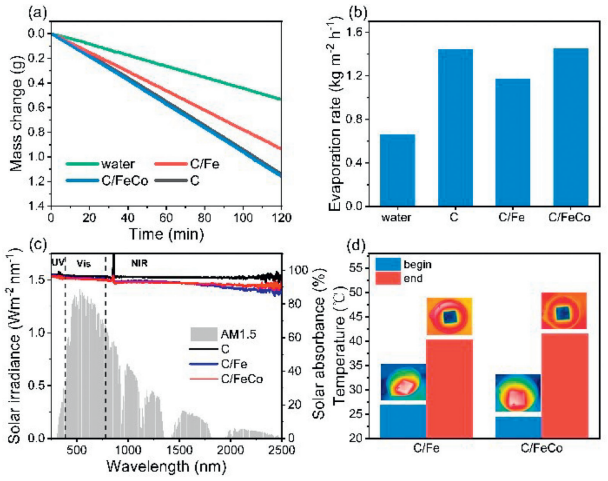

Fig. 2. (a) Mass change of water over time in different evaporators under one-sun irradiation. (b) The average evaporation rate of different evaporators. (c) Full spectra absorption of C, C/Fe, and C/FeCo membranes. (d) Average temperature of surfaces of the C/Fe membrane and C/FeCo membrane before and after 2 h of evaporation experiment. Insets show the infrared images of the top view over the samples.

taminant in the following experiments owing to its high volatilization and condensation. The initial phenol content was 10 mg/L and PDS content was 2 mmol/L in this work. We first tested the performance of C/FeCo phototherm membranes with different Fe-Co loading ratios (Fig. S1 in Supporting information). As the Fe-Co ratio was 1:2, the residual phenol in the distilled water was 0 mg/L during SIE. Therefore, the C/FeCo photothermal membrane with a Fe-Co ratio of 1:2 was finally selected for the following experiments. It can be seen from Fig. 3a that the interception efficiency of phenol for the C membrane was only 55% after 2.5 h operation. In contrast, the interception efficiency of phenol for the C/Fe membrane reached 90% after 1 h operation and slowly increased to 95% as the operation time raised to 2.5 h. Compared with C and C/Fe membranes, the C/FeCo membrane showed the highest interception efficiency, which reached 100% in 1 h and could kept stable at the following operation time. These implied that the loading of Fe and Co might endow the C membrane with a stable catalytic function. Moreover, the high catalytic efficiency of the membrane can promote more phenol in the feed solution pumping to the surface of the membrane to be degraded. The change of residual phenol concentration in feed solution over time is shown in Fig. 3b. The residual phenol concentration in feed solution began to decline from the initial 10 mg/L, but generally kept stable between 9.6 mg/L and 10 mg/L, which was similar in three types of membrane systems. The concentration of PDS in the feed solution also changed slightly during SIE (~10%, Fig. S2 in Supporting information). This indicates that after PDS was added to the original solution, the catalytic degradation of phenol did not occur in the original solution, but on the surface of the fiber membrane. As can be seen from Fig. S2 (Supporting information), the concentration of PDS remained in the feed solution for the C/FeCo membrane evaporator maintained at ~1.8 mmol/L after 1 h operation, which is much higher than that of the C/Fe membrane evaporator (~1.7 mmol/L). It indicates that the addition of Fe and Co reduced the consumption of PDS. Combined with the SEM and XRD analyses in Fig. 1, this maybe because the single metal Fe on the surface of the C/Fe membrane can be easily dissolved and transported to the feed solution through diffusion. This could activate part of PDS and result in the consumption of PDS in the bulk solution. In contrast, Fe and Co elements on the surface of the C/FeCo membrane mainly existed in the form of composite metal compounds. The ion leaching experiments illustrated that only ~0.04 wt% of Fe and ~3.5 wt% of Co were leached out under neutral and alkaline conditions with 12 h shaking (Fig. S3 in Supporting information), demonstrating the stability of the C/FeCo photothermal membrane [38]. To reveal the influencing factors of phenol interception for the C/FeCo membrane evaporator, we carried out a series of evaporation experiments. Results illustrated that phenol interception efficiency was positively correlated with solar intensity and initial PDS concentration, while negatively correlated with initial phenol concentration and feed salinity (Figs. 3c–f). It is worth mentioning that although there was salt deposition at the edge of the photothermal membrane during the brine evaporation process (Fig. S4 in Supporting information), the composite fiber membrane still had ability to remove VOC. Moreover, the interception efficiency of phenol for the C/FeCo membrane evaporator tended to be kept at a high and stable level of nearly 100% under different circumstances during the evaporation process and it remained stable in multiple cycles (Fig. S5 in Supporting information). Additionally, results of toxicity prediction for Oral Rat LD50 by T.E.S.T software (Fig. S6

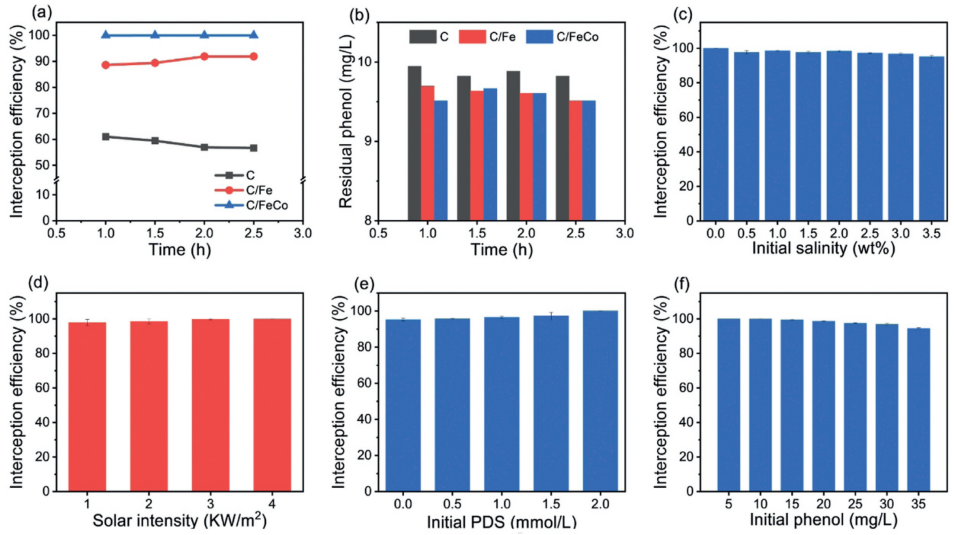

Fig. 3. (a) Phenol interception efficiency of evaporators with different photothermal membranes. (b) Comparison of residual phenol in feed solution after the evaporation of 10 mg/L phenol by different evaporators. Influence of different factors on phenol interception efficiency of C/FeCo membrane evaporator: (c) Initial salinity, (d) solar intensity, (e) initial PDS concentration, and (f) initial phenol concentration.

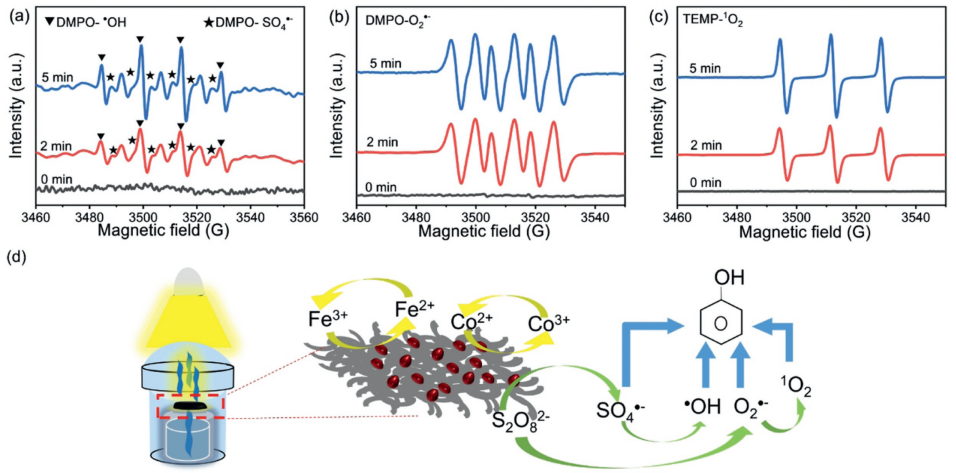

Fig. 4. ESR detection of the free radicals generated by the C/FeCo photothermal membrane with PDS mediation: (a) DMPO-•OH and DMPO-$SO_4^{•-}$, (b) DMPO-$O_2^{•-}$, and (c) TEMP-$^1O_2$. (d) Schematic illustration of the mechanism of phenol oxidation with PDS mediated C/FeCo membrane during SIE.

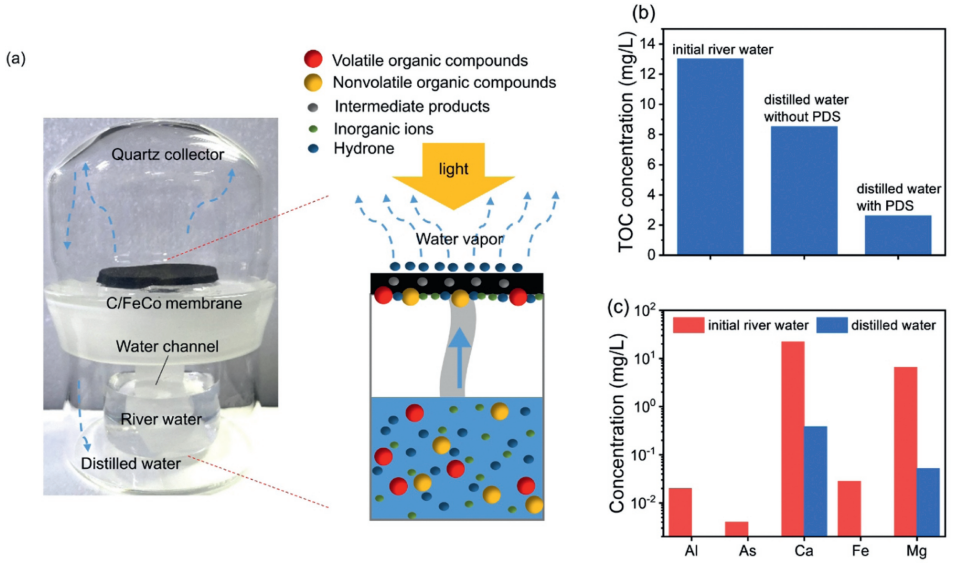

Fig. 5. (a) Digital photo and schematic illustration of the lab-made quartz distiller. (b) TOC concentration of initial river water and distilled water collected through evaporation with and without PDS. (c) Ion concentration of initial river water and distilled water.

in Supporting information) showed that the toxicity of phenol decreased greatly after degradation, enhancing the quality of the distilled water. These demonstrated that C/FeCo membrane evaporator performed excellently in VOC interception and degradation in a complex and changing environment.

To explore the mechanism of VOC interception in the C/FeCo membrane evaporator, ESR detection was carried out. As shown in Fig. 4a, four distinct •OH peaks and six distinct $SO_4^{•-}$ peaks were detected. The peaks of $O_2^{•-}$ were also intense (Fig. 4b). In addition, non-free radical $^1O_2$ in this system shows three stable peaks (Fig. 4c). The intensity of four active substances tended to increase over sunlight time. Further XPS analysis illustrated that a mixture of Fe(III)/Fe(II) and Co(III)/Co(II) coexisted in the membrane and their peak intensity slightly changed before and after reaction (Fig. S7 in Supporting information), indicating the particle compounds were the key reaction sites for PDS activation. In the catalytic oxidation process, the PDS on the surface of the C/FeCo membrane first oxidizes Co(II) to Co(III), accompanied by the formation of $SO_4^{•-}$, leading to the degradation of phenol. Given that the standard reduction potentials of Fe(III)/Fe(II) and Co(III)/Co(II) are 0.77 V and 1.83 V respectively, Fe(II) and Co(II) can be continuously regenerated as catalysts in the degradation process. It is speculated that •OH is produced by the reaction of $SO_4^{•-}$ with water. The breaking of the S-O bond of PDS produces $O_2^{•-}$. The resulting $O_2^{•-}$ may react with the •OH in the system to form $^1O_2$ [39]. To ensure the charge balance of the membrane interface, Fe(III) and Co(III) can react with active substances to generate Fe(II) and Co(II) [40]. Finally, the four active substances oxidized and degraded phenol. Thus, bimetal material realized synergistic and stable catalytic functions and ensured a continuous degradation process. Fig. 4d shows the mechanism of C/FeCo membrane in activating PDS to intercept VOC from the feed solution during the SIE process.

Natural river water often contains complex VOCs [41,42]. The VOCs in the Songhua River water are mainly naturally microbial by-products [21]. We further conducted SIE experiments using actual river water (TOC: 13.02 mg/L, Northeast, China) to evaluate the practical performance of the C/FeCo photothermal membrane (Fig. 5a). As shown in Fig. 5b, the TOC of the distilled water was 2.62 mg/L with PDS mediation, which was significantly lower than that without dosing PDS (8.53 mg/L). It suggested that this system can effectively intercept the VOCs from natural river water and reach the Drinking Water Sanitation Standard of China (GB5749–2022, 5 mg/L). To evaluate the ion interception of the SIE system, ion detection was carried out with inductively coupled plasma-

optical emission spectrometry (ICP-OES). The concentration of typical ions (*i.e.*, Al, As, Ca, Fe, and Mg) in raw river water and distilled water are shown in Fig. 5c. After SIE, the amount of inorganic ions was greatly reduced with interception efficiency all above 98%. Thus, C/FeCo photothermal membrane evaporator exhibited an effective water purification ability.

In conclusion, this work established a C/FeCo bimetallic catalytic photothermal membrane which performed excellently and stably in intercepting VOCs and producing clean water during SIE. The interception efficiency of phenol for the C/FeCo membrane evaporator reached nearly 100% during 2.5 h SIE. The catalytic oxidation mechanism of the bimetallic membrane was also revealed. For the actual river water, complex natural VOCs and inorganic ions could also be effectively purified using the C/FeCo membrane evaporator, and the distilled water met the drinking water standards of China. This work provides a simple method for intercepting VOCs during the SIE process, enlarging the application potential of SIE in water or wastewater treatment.

Declaration of competing interest

The authors declare that they have no known competing financial interests or personal relationships that could have appeared to influence the work reported in this paper.

CRediT authorship contribution statement

Yuling Ma: Conceptualization, Formal analysis, Investigation, Methodology, Project administration, Validation, Visualization, Writing – original draft. **Dongqing Liu:** Methodology, Supervision, Validation. **Tao Zhang:** Methodology. **Chengjie Song:** Methodology. **Dongmei Liu:** Resources. **Peizhi Wang:** Methodology, Supervision, Writing – review & editing. **Wei Wang:** Conceptualization, Funding acquisition, Resources, Supervision.

Acknowledgments

The authors gratefully acknowledge the National Natural Science Foundation of China (No. 52070052), National Key Research and Development Program of China (No. 2022YFB3805903), the State Key Laboratory of Urban Water Resource and Environment in HIT of China (No. 2022TS14), the National Natural Science Foundation of China (No. 52300082), the China Postdoctoral Science Foundation (No. 2023M730881), and Postdoctoral Fellowship Program of CPSF (No. GZB20230964).

Supplementary materials

Supplementary material associated with this article can be found, in the online version, at doi:10.1016/j.cclet.2024.110000.

References

[1] P. Tao, G. Ni, C.Y. Song, et al., Nat. Energy 3 (2018) 1031–1041.
[2] Z.T. Li, C.B. Wang, Chin. Chem. Lett. 31 (2020) 2159–2166.
[3] V.D. Dao, N.H. Vu, S. Yun, Nano Energy 68 (2020) 104324.
[4] Y.Q. Hou, Q.X. Wang, S.L. Wang, et al., Chin. Chem. Lett. 33 (2022) 2155–2158.
[5] F. Ni, P. Xiao, N. Qiu, et al., Nano Energy 68 (2020) 104311.
[6] T. Gao, Y. Wang, X. Wu, et al., Sci. Bull. 67 (2022) 1572–1580.
[7] S. Meng, X.J. Zha, C. Wu, et al., Nano Lett. 21 (2021) 10516–10524.
[8] Y.D. Wang, X. Wu, X.F. Yang, et al., Nano Energy 78 (2020) 105269.
[9] H. Gao, N.C. Bing, Z.J. Bao, et al., Chem. Eng. J. 454 (2023) 140362.
[10] L. Shi, Y. Shi, S. Zhuo, et al., Nano Energy 60 (2019) 222–230.
[11] J. Zhu, J. Liu, J. Liu, et al., Desalination 548 (2023) 116275.
[12] Z. Yu, R. Gu, Y. Tian, et al., Adv. Funct. Mater. 32 (2022) 2108586.
[13] L.F. Cui, P.F. Wang, H.A. Che, et al., Appl. Catal. B: Environ. 330 (2023) 122556.
[14] A.D. Nikolaou, S.K. Golfinopoulos, M.N. Kostopoulou, et al., Water Res. 36 (2002) 2883–2890.
[15] P. Wang, Environ. Sci.: Nano 5 (2018) 1078–1089.
[16] R. Chen, T. Zhang, J. Kim, et al., Environ. Sci. Technol. 55 (2021) 6248–6256.
[17] X. Ma, Z. Deng, Z. Li, et al., J. Mater. Chem. A 8 (2020) 22728–22735.
[18] J. Deng, S. Xiao, B. Wang, et al., ACS Appl. Mater. Interfaces 12 (2020) 51537–51545.
[19] J. Ma, L. An, D. Liu, et al., Environ. Sci. Technol. 56 (2022) 9797–9805.
[20] H. Mo, Y. Wang, Water Res. 226 (2022) 119276.
[21] C. Song, D. Qi, Y. Han, et al., Environ. Sci. Technol. 54 (2020) 9025–9033.
[22] D. Qi, Y. Liu, Y. Liu, et al., Adv. Mater. 32 (2020) 2004401.
[23] P. Zhang, F. Zhao, W. Shi, et al., Adv. Mater. 34 (2022) 2110548.
[24] K. Tian, L.M. Hu, L.T. Li, et al., Chin. Chem. Lett. 33 (2022) 4461–4477.
[25] G.P. Anipsitakis, D.D. Dionysiou, Environ. Sci. Technol. 37 (2003) 4790–4797.
[26] G.P. Anipsitakis, D.D. Dionysiou, Appl. Catal. B: Environ. 54 (2004) 155–163.
[27] R.H. Waldemer, P.G. Tratnyek, R.L. Johnson, et al., Environ. Sci. Technol. 41 (2007) 1010–1015.
[28] H. Zhang, C. Xie, L. Chen, et al., Water Res. 229 (2023) 119392.
[29] Z.S. Wei, F.A. Villamena, L.K. Weavers, Environ. Sci. Technol. 51 (2017) 3410–3417.
[30] R.N. Guo, Y. Chen, B.R. Liu, et al., Chin. Chem. Lett. 33 (2022) 3809–3817.
[31] C. Cai, H. Zhang, X. Zhong, et al., J. Hazard. Mater. 283 (2015) 70–79.
[32] Y. Xiao, C. Li, X. Zhou, et al., ACS ES&T Water 1 (2021) 2423–2430.
[33] D.L. Guo, S.J. You, F. Li, et al., Chin. Chem. Lett. 33 (2022) 1–10.
[34] L.F. Cui, C.W. Ma, P.F. Wang, et al., Appl. Catal. B: Environ. 337 (2023) 122988.
[35] L.F. Cui, P.F. Wang, H.A. Che, et al., Water Res. 244 (2023) 120514.
[36] Q. Yang, H. Choi, S.R. Al-Abed, et al., Appl. Catal. B: Environ. 88 (2009) 462–469.
[37] Y. Zhang, J. Wei, L. Xing, et al., Sep. Purif. Technol. 282 (2022) 120124.
[38] X. Tong, S. Ma, Y. Qi, et al., J. Taiwan Inst. Chem. Eng. 108 (2020) 64–70.
[39] T. Zhang, Y. Chen, Y. Wang, et al., Environ. Sci. Technol. 48 (2014) 5868–5875.
[40] C. Huang, H. Liu, C. Sun, et al., Environ. Pollut. 325 (2023) 121391.
[41] U.S. EPA, National Water Quality Inventory 2000 Report, US Environmental Protection AgencyOffice of Water, Washington DC, U. S. A., 2002.
[42] M.J. Moran, J.S. Zogorski, P.J. Squillace, Environ. Sci. Technol. 41 (2007) 74–81.